HAL
open science

# Revealing the Excited-State Dynamics of the Fluorescent Protein Dendra2

Eduard Fron, Mark van Der Auweraer, Benjamien Moeyaert, Jan Michiels, Hideaki Mizuno, Johan Hofkens, Virgile Adam

## To cite this version:

Eduard Fron, Mark van Der Auweraer, Benjamien Moeyaert, Jan Michiels, Hideaki Mizuno, et al.. Revealing the Excited-State Dynamics of the Fluorescent Protein Dendra2. Journal of Physical Chemistry B, 2013, 117 (8), pp.2300 - 2313. 10.1021/jp309219m . hal-01662511

**HAL Id: hal-01662511**

**https://hal.univ-grenoble-alpes.fr/hal-01662511**

Submitted on 7 Feb 2024

**HAL** is a multi-disciplinary open access archive for the deposit and dissemination of scientific research documents, whether they are published or not. The documents may come from teaching and research institutions in France or abroad, or from public or private research centers.

L'archive ouverte pluridisciplinaire **HAL**, est destinée au dépôt et à la diffusion de documents scientifiques de niveau recherche, publiés ou non, émanant des établissements d'enseignement et de recherche français ou étrangers, des laboratoires publics ou privés.

THE JOURNAL OF PHYSICAL CHEMISTRY B

Article

pubs.acs.org/JPCB

# Revealing the Excited-State Dynamics of the Fluorescent Protein Dendra2

Eduard Fron,[†] Mark Van der Auweraer,[†] Benjamien Moeyaert,[†] Jan Michiels,[‡] Hideaki Mizuno,[§] Johan Hofkens,[†] and Virgile Adam*[,†]

[†]Division of Molecular Imaging and Photonics, Department of Chemistry, Katholieke Universiteit Leuven, Celestijnenlaan 200F, 3001 Heverlee, Belgium

[‡]Centre of Microbial and Plant Genetics, Katholieke Universiteit Leuven, Kasteelpark Arenberg 20 - bus 2460, 3001 Heverlee, Belgium

[§]Laboratory of Biomolecular Network Dynamics, Division of Biochemistry, Molecular and Structural Biology, Department of Chemistry, Katholieke Universiteit Leuven, Celestijnenlaan 200G, bus 2403, 3001 Heverlee, Belgium

Supporting Information

**ABSTRACT:** Green-to-red photoconversion is a reaction that occurs in a limited number of fluorescent proteins and that is currently mechanistically debated. In this contribution, we report on our investigation of the photoconvertible fluorescent protein Dendra2 by employing a combination of pump−probe, up-conversion and single photon timing spectroscopic techniques. Our findings indicate that upon excitation of the neutral green state an excited state proton transfer proceeds with a time constant of 3.4 ps between the neutral green and the anionic green states. In concentrated solution we detected resonance energy transfer (25 ps time constant) between green and red monomers. The time-resolved emission spectra suggest also the formation of a super-red species, first observed for DsRed (a red fluorescent protein from the corallimorph species *Discosoma*) and consistent with peculiar structural details present in both proteins.

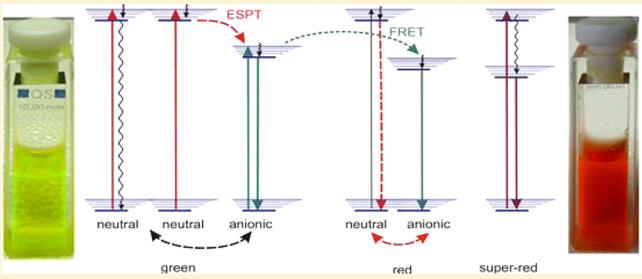


## INTRODUCTION

Dendra2 is a monomeric variant of a green-to-red photoconvertible fluorescent protein (PCFP) from the alcyonacean soft coral species *Dendronephthya*.[1] It is commonly used in fluorescence microscopy, for example, to track protein movements within living cells thanks to its more efficient green-to-red photoconversion properties compared to other similar proteins.[2−4] This photoconversion efficiency of Dendra2 is due to the exceptionally high p$K_a$ of its chromophore (7.1 and 7.5 for respectively the green and the red species), which can be explained by the particular microenvironment of this moiety.[5] Together with a good spectral separation of the absorbance and fluorescence spectra of the initial and the photoconverted form, this more efficient photoconversion makes Dendra2 an ideal reporter for live cell imaging in general and protein tracking in particular.[2,4,6] Furthermore, PCFPs are frequently used for super-resolution photoactivated localization microscopy (PALM) techniques, which allow the reconstruction of fluorescence images, based on precise localization of individual emitters, with sub-diffraction-limit resolution.[7−13] The photoconversion of green-to-red PCFPs has a complex and debatable mechanism that requires the presence of a histidine as the first amino acid of the chromophore. Although the mechanism is still prone to controversies,[14−19] it was recently proposed that this photoreaction involves a transient negative charge of this histidine (initiated by excited state proton transfer), which leads to an elongation of the chromophore's conjugation via a $\beta$-elimination.[20]

In Dendra2, the photophysics is even more complex than in other PCFPs, since a fluorescent species has been recently detected,[5,21] that is red-shifted by ∼30 nm as compared to the photoconverted red species that emits at 573 nm. A similar "super-red" (SR) species was previously reported in DsRed, a red fluorescent protein from the corallimorph species *Discosoma*.[22,23] Upon excitation of the red form of DsRed (green immature chromophores also exist in this tetrameric protein), besides the normal red fluorescent species a small and weakly fluorescent fraction that emits at wavelengths that are 15−20 nm more red-shifted is also observed. The SR species is detectable both in ensemble or single molecule spectroscopy in DsRed and its variants,[24,25] and its formation, which was proposed to proceed from the decarboxylation of the glutamate-215 along with a cis−trans isomerization of the chromophore,[26] appears to be dependent on the excitation intensity.[23] It is known that in fluorescent proteins the highly

**Received:** October 22, 2012
**Revised:** January 23, 2013
**Published:** January 28, 2013

Downloaded via CEA SACLAY on February 6, 2024 at 13:32:55 (UTC).
See https://pubs.acs.org/sharingguidelines for options on how to legitimately share published articles.

 © 2013 American Chemical Society 

conserved glutamate located in the vicinity of the chromophore can undergo a decarboxylation reaction upon strong illumination. The decarboxylation is preceded by a photoinduced electron transfer from glutamate to the chromophore.[26−29] Such a decarboxylation furthermore clearly involves an excited state proton transfer from the glutamate to the chromophore and always leads to modifications in the fluorescence properties. Depending on the fluorescent protein, this photoinduced decarboxylation indeed induces phototransformation processes, resulting, for example, in bathochromic shifts for the wild type GFP[27,29,30] or photoactivatable fluorescent proteins.[31−33] In some other cases, a shift to shorter wavelengths[34] or a destabilization of the chromophore associated with the glutamate decarboxylation has been observed.[35−38] Raman studies by Habuchi et al. in DsRed are unambiguously consistent with a structural modification of the chromophore during the formation of the SR species.[26] However, it is uncertain whether a large amplitude structural modification such as a cis−trans isomerization is necessary to observe the SR species. Bonsma and co-workers showed, for example, that the formation of the SR species in DsRed could be obtained at temperatures as low as 1.6 K.[39] It seems more likely that a more planar chromophore reached by an isomerization or by the cryotrapping of a favorable conformation leads to a more complete conjugation and gives rise to red-shifted emissions.

It is, however, questionable if such reversible formation of the SR species can involve the irreversible photo-Kolbe reaction at glutamate-215. Here, we report a systematic investigation on the photophysics and excited state dynamics of Dendra2 in solution upon excitation of both neutral and anionic species. Given the short distances between the protein constituents, many of the intramolecular processes that are important in photoconversion are expected to be governed by fast processes that can only be probed by ultrafast spectroscopy. Femtosecond fluorescence up-conversion, transient absorption, and time-correlated single photon counting (TCSPC) techniques were employed to unravel the possible relaxation pathways following excitation. In addition, steady-state spectroscopy was used to determine the presence of certain species and their fluorescence properties. The experimental results were compared with those obtained from proteins with analogous photoconversion properties.

## ■ EXPERIMENTAL SECTION

**Synthesis of Materials.** Dendra2 was expressed from the pRSET vector (Invitrogen) in *Escherichia coli* JM109(DE3) cells (Promega, Madison, WI). Recombinant protein was prepared as described by Mizuno et al.[40] Briefly, transformed bacteria were grown in LB medium, and protein production was induced by IPTG. Cells were disrupted by freeze−thaw cycles, and the hexahistidine-tagged protein was purified using Ni-NTA agarose (Qiagen).

**Stationary Experiments.** The stationary measurements were recorded using a spectrophotometer (Lambda 40, Perkin-Elmer) and a fluorimeter (SPEX Fluorolog-3, Horiba- Jobin Yvon) corrected for the wavelength dependence of the detection system.[41] The optical density at the absorption maximum of all samples was kept below 0.1 in a 1-cm cuvette at the excitation wavelength.

**Picosecond Fluorescence Time-Correlated Single Photon Counting Experiments.** The fluorescence decay times were determined by TCSPC measurements, and the setup has been described in detail previously.[42] A time-correlated single photon timing PC module (SPC 830, Becker & Hickl) was used to obtain the fluorescence decay histogram in 4096 channels. The decays were recorded with 10 000 counts in the peak channel, in time windows of 15 ns corresponding to 3.7 ps/channel, and analyzed globally with time-resolved fluorescence analysis (TRFA) software.[43,44] The full width at half-maximum (fwhm) of the IRF was typically on the order of 40 ps. The quality of the fits was judged by the fit parameters $\chi^2$ (<1.2), $Z\chi^2$ (<3), and the Durbin Watson parameter (1.8 < DW < 2.2), as well as by the visual inspection of the residuals and autocorrelation function.[45] All measurements were performed in cuvettes with an optical path length of 1 cm at an optical density of ca. 0.1 at the excitation wavelength of 375 nm.

**Femtosecond Time-Resolved Experiments.** *Fluorescence Up-Conversion Experiments.* An amplified femtosecond double OPA (optical parametric amplifier) laser system that has been described previously was used.[46] The power of the excitation beam was set to 150 $\mu$W (which corresponds to 150 nJ/pulse) and the fluorescence light emitted from the sample was efficiently collected using a Cassegrain objective. The fluorescence was then filtered using a long pass filter for suppressing the scattered light, directed and overlapped with a gate pulse (800 nm, ca. 10 $\mu$J) derived from the regenerative amplifier onto an LBO crystal. By tuning the incident angle of these two beams relative to the crystal plane, the sum frequency from the fluorescence light and the gate pulse was generated. The time-resolved traces were then recorded by detecting this sum frequency light while changing the relative delay of the gate pulse versus the sample excitation time. Fluorescence gating was done under magic angle conditions in a time window of 50 ps. As detector, a photomultiplier tube (R1527p, Hamamatsu) placed at the exit of a 30-cm monochromator was used (heterodyne mode, vide infra). An additional bandpass filter was placed in front of the monochromator to allow only the sum frequency light to enter. The electrical signal from the multiplier tube was gated by a boxcar averager (SR 520, Stanford Research Systems) and detected by a lock-in amplifier (SR830, Stanford Research Systems). The prompt response of this arrangement (including laser sources) was determined by detection of scattered light under otherwise identical conditions and found to be approximately 250 fs (fwhm). This value was used in the analysis of all measurements for curve fitting using iterative reconvolution of the data sets. Global analysis of the fluorescence decays obtained at different wavelengths as a sum of exponentials allowed us to obtain decay associated spectra (DAS). When interpreting the features of those DAS, one should keep in mind that no correction for the wavelength dependence of the sensitivity of the detection setup (mixing crystal, filters, PMT) was applied. The sample was prepared in a concentration that yielded an absorbance of ca. 0.4 per mm at the excitation wavelength and was contained in a quartz cuvette with an optical path length of 1 mm. During the measurements of the green form, the sample was kept continuously flowing to avoid photoconversion as well as irreversible photodegradation. To improve the signal-to-noise ratio, every measurement was averaged 15 times at 256 delay positions, where a delay position is referred to as the time interval between the arrival of the pump and the gate pulses at the sample position. After each experiment the integrity of the samples was checked by recording the steady state absorption and emission spectra and comparing them with those obtained before the experiments. Although after a number of experiments the sample underwent

photoconversion, no spectral changes suggesting photodegradation were observed.

*Femtosecond Transient Absorption Measurements.* The experiments were performed with the same amplified femtosecond double OPA laser system, providing an intense pulse (150 $\mu$J) used for excitation (395 nm) and a weak pulse used for probing the changes in absorption in a wavelength range between 470 and 770 nm.[46] The probe light was generated by focusing an 800-nm beam in a 3-mm sapphire plate to obtain a white light continuum into the visible region. The monochromatic detection (heterodyne mode) was performed using a PMT (R1527p, Hamamatsu) placed at the second exit of the spectrograph mounted behind a slit. The pulse duration was 250 fs (fwhm) at the sample position, as determined by cross correlation, and the measurements were performed at the magic angle conditions (54.7° relative orientation between the pump and probe light polarization planes). During the measurements, the sample was kept continuously flowing to avoid photoconversion as well as irreversible photodegradation. Some additional transient absorption experiments (see Figure S7 of the Supporting Information and discussion thereafter) have been performed at a later stage with a different setup that confers a time resolution of 100 fs.

*PMT Detection/Heterodyne Mode.* Optical heterodyne detection is a highly sensitive technique to measure weak changes in absorption induced by a frequency-modulated pump beam. The electrical signal from the photomultiplier tube was gated by a boxcar averager (SR 250, Stanford Research Systems) and detected by a lock-in amplifier (SR830, Stanford Research Systems). We only detect the amplitude of the signal (ignoring the phase) which is always positive. The sign of the amplitude has been assigned on the basis of the signals detected with the CCD camera. Single traces and global analysis were carried out using Origin's nonlinear least-squares fitter (Originlab, Northampton, MA). A test (multi)exponential function convoluted with a Gaussian of 250 fs (representative of the instrument response function) is optimized to fit the experimental data sets. The quality of the fits was judged by the reduced $\chi^2$ values (within a given data set) as well as by visual inspection of the residuals.

## ■ RESULTS AND DISCUSSION

**Steady State Measurements.** The absorption, excitation, and emission spectra of green, red, and partially photoconverted Dendra2 samples are shown in Figure 1.

*Green Dendra2.* At pH 7.4 the absorption spectrum of green Dendra2 (Figure 1A) consists of two bands with maxima at 385 and 490 nm that are known to correspond to the neutral and anionic form of the chromophore, respectively.[5] The intensities of these bands are pH-dependent: at high (low) pH values the intensity of the 490-nm band increases (drops off), whereas that of the 385-nm band drops off (increases), as shown in Figure S9 (Supporting Information). The excitation of the anionic chromophore of green Dendra2 produces a typical intense and relatively narrow GFP-like emission spectrum with a maximum at 505 nm and a faint shoulder at ~550 nm (Figure 1D), in agreement with literature data.[5] Similar spectra are obtained upon 375 and 395 nm excitation with intensity maxima proportional to the absorption at these wavelengths. The excitation spectra of green Dendra2 recorded at 505 nm shows a contribution of the absorption band of the neutral green species that is much smaller than the contribution of this species to the absorption spectrum. This suggests that if excited

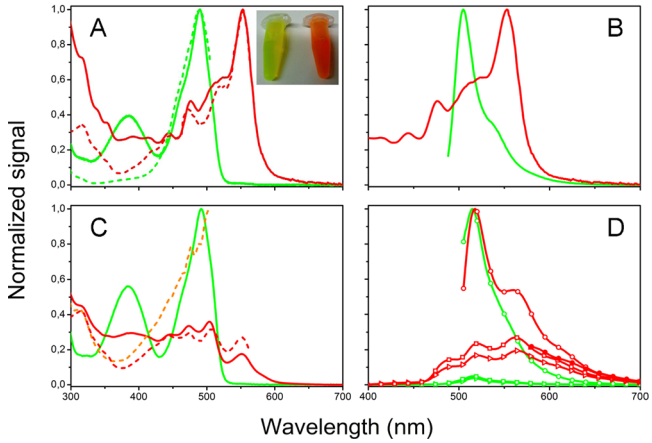


**Figure 1.** Steady-state spectra of Dendra2 at pH 7.4. (A) Absorption (solid) and excitation (dashed) spectra of green ($\lambda_{em}$ = 515 nm) and red ($\lambda_{em}$ = 573 nm) solutions. (B) Spectral overlap between the emission spectrum of the green form ($\lambda_{exc}$ = 480 nm) and the absorption spectrum of the red form. (C) Plain lines show the absorbance spectra of the green and partially photoconverted species (green and red, respectively). Dashed lines depict the excitation spectra of the red species at $\lambda_{em}$ = 515 nm (orange) and at $\lambda_{em}$ = 573 nm (red). (D) Emission spectra of the green and red species are shown as green and red lines, respectively at $\lambda_{exc}$ = 375 nm (open triangles), $\lambda_{exc}$ = 395 nm (open squares), $\lambda_{exc}$ = 495 nm (open circles), and $\lambda_{exc}$ = 570 nm (closed circles). Inset: photographs of tubes containing green and partially photoconverted red Dendra2 under ambient light.

state proton transfer (ESPT) occurs, its quantum yield does not exceed 0.1−0.2.

The absorption spectrum at pH 7.4 of the sample referred to in this study as partially photoconverted Dendra2 (the photoconversion was done by irradiating the sample with 395-nm light, Figure 1A solid red) is composed of several bands. This is essentially a superposition of a small fraction of green Dendra2 (bands at 385 and 490 nm as described above) and a large fraction of red Dendra2. The latter is characterized by a main peak at 556 nm and by a vibronic shoulder at 516 nm and a second band located at 470 nm accompanied by a vibronic progression at 440 nm. Similar to the green form, these two bands are associated with the electronic transitions of the anionic red (553 and 516 nm) and neutral red (470 and 440 nm) forms of the chromophore.[5] The additional signal observed in the 300−350 nm region is probably due to transitions to higher excited electronic states of this red chromophore. In contrast to the green form, excitation spectra of the red Dendra2 recorded at 573 nm indicates that both neutral and anionic species contribute appreciably to the fluorescence emission. This corresponds to the observations of Adam et al.,[5] who found fluorescence quantum yields of respectively 0.45 and 0.61 for the neutral red (pH 5) and anionic red form (pH 9).

*Red Dendra2 Emission.* The fluorescence emission spectra of the partially photoconverted red Dendra2 have a complex character. As seen in Figure 1 D, at 495-nm excitation the emission spectra consist of two bands: a green band with maximum at 505 nm and a red one with maximum at 573 nm associated with the fluorescence of the green and red forms of Dendra2 present in the sample, respectively. Upon 375- or 395-nm excitation, we noticed an additional band centered at 480 nm eventually related to the fluorescence of the directly excited

neutral green or neutral red chromophore. The much larger fluorescence quantum yield of neutral red[5] compared to neutral green and the fact that the position of this maximum corresponds better with that of the neutral red (481 and 517 nm) than with that of neutral green (454 nm) suggest that this band has to be attributed to the neutral red rather than to the neutral green chromophore. Excitation at 570 nm produces the pure emission spectra of the red Dendra2 attributed to the radiative deactivation of the anionic species (see Figure 1D or 3A).

**Time-Resolved Absorption and Fluorescence Experiments.** In order to study the excited state processes responsible for photoconversion reaction and potential intermediate species formed in Dendra2, we investigated the evolution of the excited and ground states after excitation through a series of femtosecond fluorescence up-conversion, transient absorption, and time-correlated single photon counting (TCSPC) experiments selectively exciting the neutral and anionic species of the green and red chromophore of the protein.

**TCSPC Experiments.** *Green Dendra2.* The time-dependent fluorescence properties of the anionic species of green Dendra2 at 495 nm excitation on the nanosecond time scale have been earlier investigated, and the fluorescence was found to decay monoexponentially with a time constant of 3.3 ns.[21] Quite intriguing, we observed that when a solution of pH 7.4 of green Dendra2 (where both the neutral and anionic species are present) is excited with wavelengths around or shorter than 400 nm, the kinetics is no longer monoexponential: at 375-nm excitation the decay traces obtained by TCSPC had to be analyzed as a sum of four exponentials. Figure S1 (Supporting Information) displays the wavelength dependence of the relative amplitudes of the different components, and Table 1 compiles the time constants retrieved upon analysis of the traces. Beside a component of 3.3 ns, responsible for most of the stationary emission related to the anionic species, two smaller components with decay times of 500 and 200 ps and similar wavelength dependences were observed.[47] These minor components were attributed to a fraction of the molecules where extra nonradiative decay channels are present. Furthermore, a component with a decay time of about 60 ps was observed at wavelengths between 450 and 475 nm, situated in the blue part of the absorption spectrum. At this point, a tentative attribution of this component would be purely speculative, as the recovered value of the decay time is close to the fwmh of the IRF of our TCSPC setup.

**Table 1. Decay Time Constants and Wavelengths Where Their Relative Amplitudes Reach a Maximum As Obtained by TCSPC for Green Dendra2 Excited at 375 and 495 nm at pH 7.4[a]**

| $\lambda_{exc}$/nm | green form decay time/ps (max wavelength/nm) | | | | | |
|---|---|---|---|---|---|---|
| 375 | 60 (450) | 200 (530) | 500 (530) | – | – | 3300 (530) |
| 495[15] | – | – | – | – | – | 3300 |

[a]Dashes indicate that values are not observed.

**Femtosecond Fluorescence up-Conversion Experiments.** The complex kinetics observed upon 375-nm excitation and the intriguing component of 60 ps motivated us to look at the fluorescence decay on a shorter time scale by employing femtosecond up-conversion experiments, as this setup can detect components as fast as 250 fs.

*Green Dendra2.* The fluorescence decays (time window of 420 ps) obtained upon excitation at 375 nm of a pH 7.4 solution of green Dendra2 can be analyzed at 450 and 475 nm as the sum of two exponentials with a decay time of 40 and 3.4 ps and a nearly identical amplitude (Table 2). For the analysis of the fluorescence decay at 515 nm, obtained under identical conditions, a third component with a decay time equal to or longer than 500 ps and an amplitude of 24% is necessary (see Figure S8, Supporting Information). Considering the data obtained with TCSPC the decay time of this component was kept fixed at 3300 ps during the analysis of the fluorescence decays. While the 40-ps component corresponds to the 60-ps component recovered from the TCSPC experiments (considering the experimental error in the latter experiment) the 3.4-ps component could not be observed at all using TCSPC. The fact that the ratio of the amplitudes of the 3.4- and 40-ps components changes only little from 450 to 515 nm suggests that both components correspond to two different populations of the same species, probably the neutral green chromophore, while the component at 515 nm with a decay time of 500 ps or longer can be attributed to the anionic green chromophore.

*Partially Photoconverted Red Dendra2. 570-nm Excitation.* The fluorescence decay of the red form of the protein contained in a partially photoconverted sample at pH 7.4 recorded upon 570-nm excitation (where only the red anionic species absorbs) revealed three decay components of 320 fs and 15 ps and one ≥50 ps, which was kept fixed at 4400 ps (Figure S2, Supporting Information) considering the fact that for the anionic red state a fluorescence decay of 4.4 ns was observed earlier.[5] The 4400-ps component has the largest amplitude (70% at 590 nm) and, based on the corresponding DAS which was red-shifted compared to the green form, can be straightforwardly attributed to the fluorescence decay of the red anionic species. The DAS of the 320-fs component (26% at 590 nm) has positive amplitude at short wavelengths and negative amplitude at longer wavelengths, which is also clearly

**Table 2. Decay Time Constants and Wavelengths and Wavelengths Where Their Relative Amplitudes Reach a Maximum As Obtained by Fluorescence Up-Conversion Experiments for Dendra2 for 375, 495, and 570 nm Excitation Wavelength at pH 7.4[a]**

| $\lambda_{exc}$/nm | decay time/ps (max wavelength/nm) | | | | | | | | | | | |
|---|---|---|---|---|---|---|---|---|---|---|---|---|
| | green form | | | | | | green + red forms | | | red form | | |
| 395 | 1.8 (600) | 2.7 (520) | 3.4 (500) | 25 (530) | 40 (490) | 3500 (550) | 2.67 (570) | 25 (520) | 3500 (550) | – | – | – |
| 495 | 0.420 (510) | – | – | – | – | 3300 (530) | – | – | – | – | – | – |
| 570 | – | – | – | – | – | – | – | – | – | 0.320 (590) | 15 (610) | 4400 (590) |

[a]Dashes indicate that values are not observed. The long components (3300, 3500, and 4400 ps) were kept fixed during the fit analysis.

seen upon visual inspection of the decays (Figure S2A, Supporting Information). This suggests a relaxation process (vibrational relaxation or intramolecular vibrational distribution). Furthermore, there is also a small (4% at 590 nm) component with a decay time of 15 ps. Since the amplitude of this component is small and thus insufficiently clear to see its wavelength dependence with sufficient accuracy, we can only speculate on its nature. Such component may possibly indicate a slow conformational relaxation in the excited state of the chromophore.

*395-nm Excitation.* Excitation at 395 nm of this partially photoconverted sample results in a fluorescence decay (Figure 2) which could be analyzed as a sum of three exponentials with

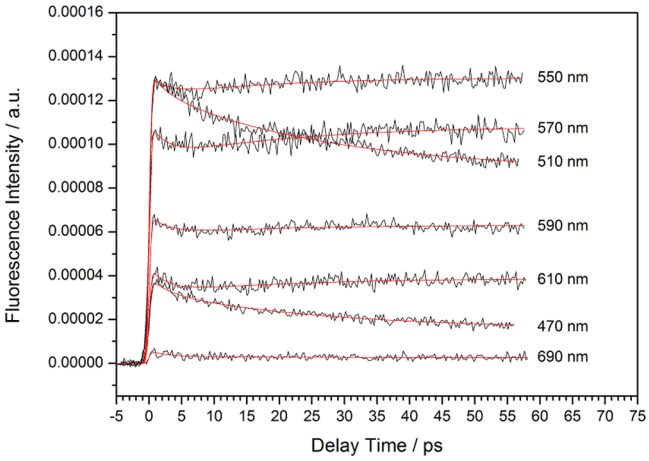


**Figure 2.** Sample of decay traces and the corresponding fits obtained for partially red photoconverted Dendra2 by femtosecond fluorescence up-conversion technique in 50 ps time window ($\lambda_{exc}$ = 395 nm, $\lambda_{det}$ = 450−690 nm, pH 7.4).

decay times of 2.7, 25, and 3500 ps (the long component was kept fixed during the fit analysis) with amplitudes spectrally distributed between 450 and 690 nm as shown in Figure 3 (see Figure S3 of the Supporting Information for the complete set of decay traces). Figure 3 displays the emission spectra of the green and red forms and the DAS of these time components. The DAS of the 3.5-ns contribution is compatible with a sum of the amplitudes of the green (3.3 ns) and red (4.4 ns) forms that cannot be distinguished in the time window of this experiment. The small shoulder below 500 nm can be attributed to the neutral red species which, according to the reported fluorescence quantum yield,[5] will also have a fluorescence decay in the nanosecond range. The DAS of the fastest component of 2.7 ps is characterized by small amplitudes that are spread over both green and red emission regions and can be linked to relaxation processes such as vibrational relaxation.[48] As the amplitude of this component is always small, it will not be discussed in more detail. An interesting wavelength dependence can be observed for the DAS of the 25-ps component, as it changes its sign from positive (decay), in the emission region of the green form, to negative (rise) in the emission region of the red form. Such DAS is characteristic of and suggests the occurrence of energy transfer (FRET) from the excited state of the green anionic to the red anionic species in the partially photoconverted sample. We need to emphasize that, in order to obtain qualitative femtosecond experiments, the sample was primed at a relatively high concentration of about 233 $\mu$M to yield a necessary OD of 0.4 at the excitation

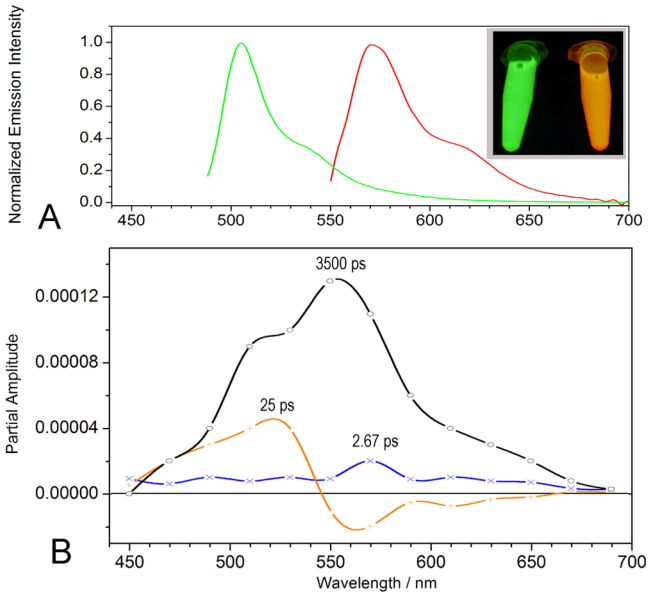


**Figure 3.** (A) Stationary emission spectra of green (green) and red (red) Dendra2 recorded with $\lambda_{exc}$ = 488 nm and $\lambda_{exc}$ = 540 nm, respectively. (B) Decay associated emission spectra of partially photoconverted red Dendra2 obtained by femtosecond fluorescence up-conversion technique in a 50-ps time window ($\lambda_{exc}$ = 395 nm, $\lambda_{det}$ = 450−690 nm, pH 7.4); the 3500-ps component was kept fixed during the fit analysis. Inset: photographs of tubes containing fluorescent green and partially photoconverted red Dendra2.

wavelength. At this elevated concentration, the probability of dimer formation increases significantly (vide infra).

**Transient Absorption Experiments.** To further underpin our observations, we performed a series of transient absorption experiments with the aim of observing the evolution of the ground state population of the red anionic species. The pH 7.4 solution of a partially red Dendra2 was excited at 495 nm, which is close to the maximum of the absorption of the green anionic form, although also the neutral and anionic red forms show significant absorption at this wavelength.[5] The signals between 550 and 610 nm could be fitted by a triple exponential function with decay times of 0.5, 25, and 4400 ps (the latter kept fixed considering the observed fluorescence decay time of the red anionic state).[5] The negative sign of the DAS associated with the latter component and the agreement of its spectral features with the absorption and emission spectrum of the red anionic form suggest that it is due to the depletion of the ground state and/or induced emission (see Figure S4, Supporting Information). Furthermore, visual inspection of the signal at 570 nm clearly shows an increase of this depletion and/or induced emission with a time constant on the order of a few tens of picoseconds that would correspond with the DAS of the 25-ps component, which has a positive contribution at ∼570 nm (Figure S4B, Supporting Information). This means that a fraction of the excited anionic red species is not populated immediately upon excitation but originates from another excited species with a decay time of 25 ps that can be excited at 495 nm. Once more, it is reasonable to attribute this 25-ps component to a FRET from the initially excited green anionic form or neutral red form to the red anionic form. At 550 nm this component nearly disappears because the decay signal of the induced emission of the green anionic form is nearly canceled by the rise signal of the depletion of the ground state of the red anionic form. Finally, the features of the DAS of

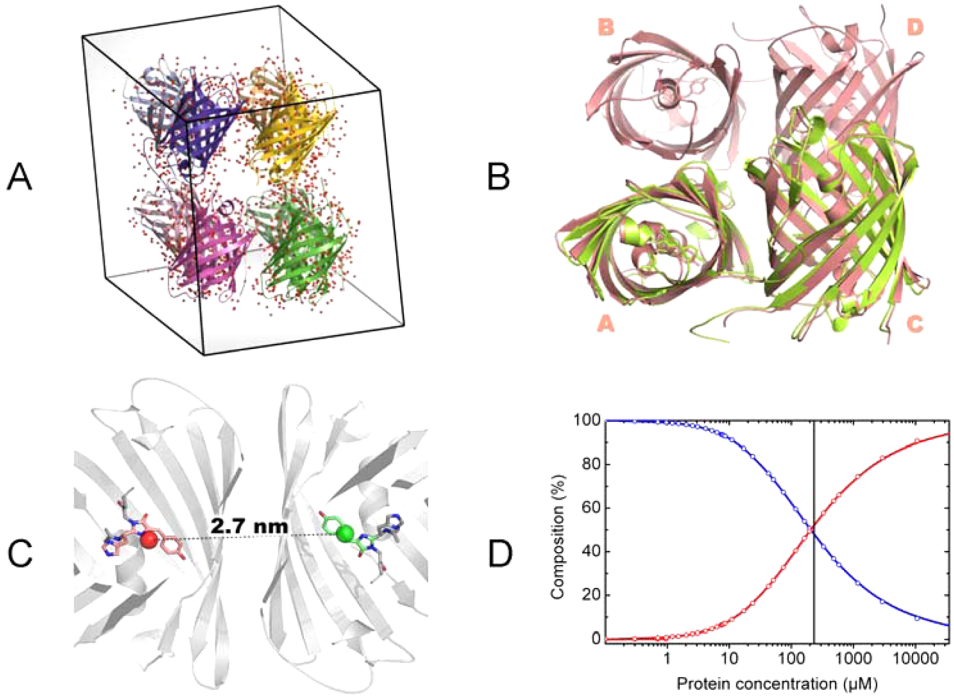


**Figure 4.** Dimeric organization of Dendra2. (A) The asymmetric unit of a crystal of Dendra2 contains four dimers, each separated from the neighboring ones by several shells of water molecules (red spheres). (B) Dimers of Dendra2 (green, PDB code 2VZX) superpose with the chains A and C of the tetrameric DsRed (salmon, PDB code 1ZGO) with a rmsd for all atoms of 1.08 Å. (C) The average distance between the centers of mass (balls) between a green and a red chromophore (sticks) of respective chains (cartoon) in a dimer of Dendra2 is ~2.7 nm. (D) The ratio of monomers (blue) and dimers (red) relative to protein concentration of Dendra2 is indicating an equivalent distribution of the two populations at 233 $\mu$M.

the 500-fs signal are compatible with vibrational relaxation of the red anionic form excited at 495 nm. The occurrence of FRET is also supported by the extensive overlap between the emission spectrum of the green and the absorption spectrum of the red anionic species (Figure 1B) or between the neutral and anionic red species.[5] Such a FRET process was also reported to occur in other green-to-red photoconvertible fluorescent proteins like Kaede[49] or between green immature and red mature chains of DsRed.[23,50−53] As experimentally proven above, the excitation energy transfer seems to take place between two adjacent proteins in solution upon the formation of dimers at the concentrations used in transient absorption measurements. To find whether such conditions occur, we need a closer look at the probability of dimer formation in which Förster-type singlet−singlet interaction can take place.[54]

*Formation of Dimers and FRET.* As previously described,[5] several amino acids (Glu-96, Thr-143, Arg-149, Asn-158, and Arg-216) stabilize the formation of a dimeric arrangement of Dendra2 molecules when the protein concentration increases. This arrangement is clearly observable in the crystal structure of Dendra2 (PDB ID 2VZX), where four identical dimers are present in the asymmetric unit (Figure 4A). Compared to the typical tetrameric arrangement of anthozoan fluorescent proteins, in which each chain labeled from A to D forms two types of interfaces called A/B (or C/D) and A/C (or B/D),[55] the dimers formed in Dendra2 are all of the A/C type[5] and superimpose to a large extent (rmsd = 1.08 Å) with the chains A and C of the very well characterized tetramer of DsRed (Figure 4B). The interchromophoric distance in this dimer is 2.7 nm (Figure 4C) and an orientation factor $\kappa^2 = 1.64$ between these chromophores has been measured in DsRed[52] and used for other FPs such as Kaede and HcRed.[49,56]

At concentrations used in this study (233 $\mu$M), our analytical ultracentrifugation measurements[21] showed that the molecules are in equilibrium between monomers and dimers in equal amounts (see Figure 4D). We also determined in other studies that the fluorescence quantum yield of the anionic green form of Dendra2 at pH 7.4 is 0.55 and that the extinction coefficient of the anionic red form is 36 200 $M^{-1}$ $cm^{-1}$ at the absorption maximum. With these data and eq 1,[57] we calculated a value of 6.0 nm for the Förster radius $R_0$, the distance at which the FRET from the green to the neighboring red chromophore of the same dimer occurs with 50% probability.

$$R_0 = 0.02108\left(\frac{\kappa^2\Phi_D}{n^4} \times \int_0^\infty I_D(\lambda)\,\varepsilon_A(\lambda)\lambda^4\,d\lambda\right)^{1/6} \quad (1)$$

$N_A$ is Avogadro's number, $n$ is the refractive index commonly assumed to be 1.4 for biomolecules, $\kappa^2$ is the orientation factor (1.64), $\Phi_D$ is the fluorescence quantum yield of the donor in the absence of transfer, $I_D(\lambda)$ is the normalized spectral radiant intensity to unit area of the donor so that $\int I_D(\lambda)\,d\lambda = 1$, and $\varepsilon_A(\lambda)$ is the molar absorption coefficient of the acceptor expressed in $M^{-1}$ $cm^{-1}$. The obtained Förster radius of 6.0 nm is clearly longer than the interchromophoric distance, indicating a FRET efficiency above 99%. According to eq 2 and considering the decay time of the donor in the absence of the acceptor ($\tau_D$ = 3.3 ns) obtained by TCSPC, a value of 27 ps is calculated for the time constant of energy transfer ($\kappa_T = 36.5 \times 10^9$ $s^{-1}$), which corroborates with the value of 25 ps experimentally observed in femtosecond fluorescence up-conversion and transient absorption measurements.

$$1/k_T = \tau_D(R/R_0)^6 \quad (2)$$

As Dendra2 has an exceptionally high p$K_a$ for a FP[5] (p$K_a$ = 7.1 for the green species and 7.5 for the red species), at the physiological pH used in this study (pH 7.4), the neutral fraction is not negligible.

**Photoconversion of Green Dendra2.** *Fluorescence Up-Conversion Experiments.* To investigate the irreversible photoconversion mechanism that occurs upon the illumination of the protein by UV light, sequences of femtosecond up-conversion experiments have been conducted. Both neutral and anionic species of the chromophore were excited using 495- and 395-nm laser wavelengths, respectively.

The fluorescence decay traces of the green Dendra2 form recorded upon 495 nm excitation at pH 7.4 could be analyzed as biexponential decays. A slow-decaying component of which the decay time was fixed to 3.3 ns (fluorescence decay time of the anionic green form as determined by TCSPC) and a fast-decaying one of 420 fs with negative amplitude were obtained (Figure S5, Supporting Information). The DAS (Figure S5B, Supporting Information) and literature reports[21] suggest that the long component can be attributed to the excited state fluorescence decay of the green anionic form, whereas the ultrafast component showing a negative amplitude can be attributed to a relaxation process specific for the intramolecular vibrational redistribution or vibrational relaxation.[48]

The excitation of the neutral green species at 395 nm reveals a rather complex excited state dynamics. It needs to be mentioned here that, in spite of the sample being kept under continuous flow during these experiments, a certain amount of sample underwent green-to-red photoconversion. Figure 5 displays a few decay traces with their corresponding fits (the full set is shown in Figure S6, Supporting Information) and Figure 6 the corresponding DAS found upon global analysis of these traces. Global analysis of the decays obtained between 450 and 690 nm over a time interval of 60 ps needed five components with decay times of 1.8, 2.7, 3.4, 40, and 3500 ps (the 3500-ps component was kept fixed during the fit analysis). When we tried to do the curve fitting of the up-conversion data while replacing the 2.7- and 3.4-ps components with a single component, we obtained fits that were significantly worse, especially toward the blue end of the range investigated. This suggests that while the 3.4-ps component is rather related to the decay of part of the neutral green molecules (those undergoing ESPT), the 2.7-ps component has to be attributed to other species emitting at longer wavelengths. One should note that the decay times of 3.4 and 40 ps and a decay time longer than 500 ps were also retrieved for fluorescence decay traces of the green species obtained in a time interval of 420 ps for a wavelength range of 450−515 nm (Figure S8, Supporting Information) upon excitation of the green Dendra2 at 375 nm. The component with the 40-ps decay time is probably due to the species yielding the 60-ps component (which is close to the limit of the time resolution of TCSPC, see Experimental Section) of the fluorescence decay of the green form obtained by TCSPC upon excitation at 375 nm and at pH 7.4 (Figure S1, Supporting Information). When comparing the DAS of these components with the emission spectrum of the neutral green species,[5] the 3.4-ps as well as the 40- (60-)ps component can be attributed to the neutral green species. The slight red shift of the DAS as determined by the up-conversion experiment can be attributed to the wavelength dependence of the sensitivity of the detection setup. To further study this component, we have measured a series of absorption and emission spectra on Dendra2 and on a variant of Dendra2 that we recently engineered, called NijiFP,[21] (see Figure S9, Supporting Information). At pH 7.4 and upon excitation at 488 nm, the only observable fluorescence comes from the anionic species for both proteins (∼500 nm). Upon excitation at 375 nm, where the anionic peak is still dominant in the fluorescence spectrum, we can notice a shoulder at ∼450 nm in the fluorescence spectrum that is more pronounced in Dendra2, whose chromophore has a higher p$K_a$ than NijiFP. At a lower pH (6.0) and upon excitation at 375 nm, the signal at ∼450 nm is clearly visible, here again in a more pronounced way for Dendra2. These results demonstrate that the neutral Dendra2 green molecules emit at ∼450 nm and strongly suggest that the 40-ps component measured at this wavelength corresponds to this neutral fraction.

The DAS of the 3500-ps component, which extends more to the red than that of slow decaying component of the anionic green excited at 495 nm (Figure S5, Supporting Information), can be regarded as a combination of the amplitudes of the anionic green (3300 ps) and red (4400 ps) forms that cannot be discriminated in the time scale of the experiment (50-ps window). Considering that the emission spectrum of the

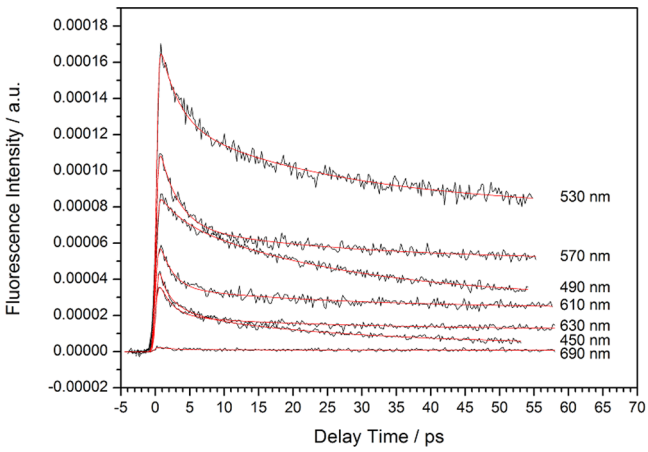


**Figure 5.** Sample of decay traces and corresponding fits obtained for green Dendra2 by femtosecond fluorescence up-conversion technique in a 50-ps time window ($\lambda_{exc}$ = 395 nm, $\lambda_{det}$ = 450−690 nm, pH 7.4).

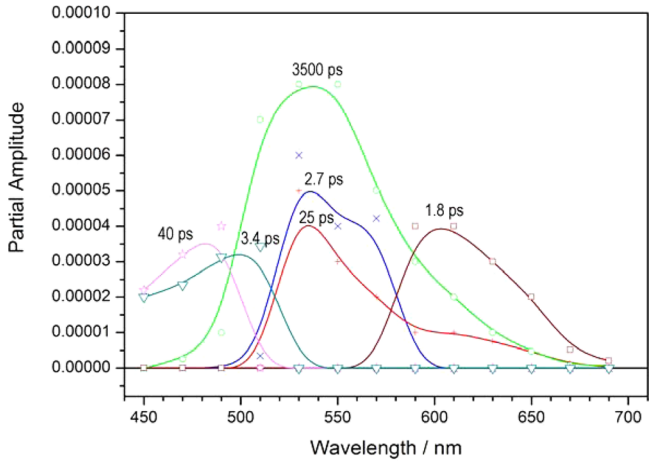


**Figure 6.** Decay associated emission spectra obtained for green Dendra2 by femtosecond fluorescence up-conversion technique in a 50-ps time window ($\lambda_{exc}$ = 395 nm, $\lambda_{det}$ = 450−690 nm, pH 7.4). The 3500-ps component was kept fixed during the fit analysis.

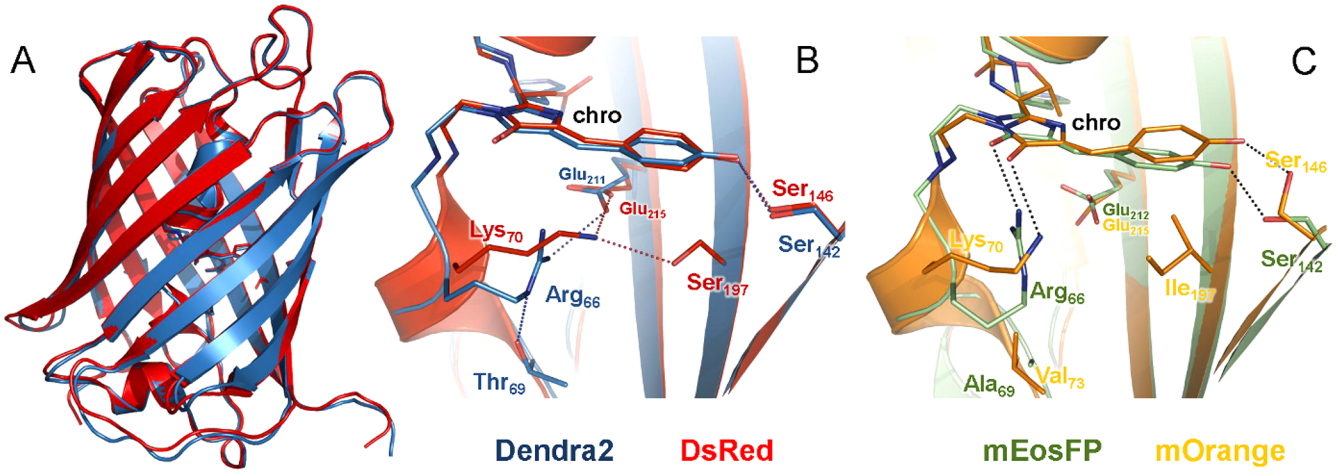


**Figure 7.** A common structural feature between DsRed and Dendra2. (A) Superposition of the overall structures of DsRed (red, PDB code 1ZGO) and Dendra2 (blue, PDB code 2VZX). (B) A closeup of the chromophore and surrounding key residues in DsRed and Dendra2. (C) A closeup of the same region in mOrange (orange, PDB code 2H5O) and another photoconvertible fluorescent protein, mEosFP (green, PDB code 3P8U). Dotted lines represent the H-bonds (less than 3 Å). For a more complete description, see Figure S10 of the Supporting Information.

neutral red species is quite similar[5] to that of the anionic green species and that on the basis of its fluorescence quantum yield of 0.45[5] this neutral red species can have a decay time of several hundreds of picoseconds up to several nanoseconds, it cannot be excluded that the blue tail of the spectrum of the 3500-ps component is to some extent also due to the neutral red species. One should note that the 200- and 500-ps components observed by single photon timing upon excitation of the neutral green form at 375 nm are not recovered here. This could be due to the fact that in a time window of 55−60 ps it is not possible to discriminate between a decay time of 200 ps, 500 ps, and several nanoseconds. The presence of the anionic red emission in the DAS of a sample of green Dendra2 is due to the high photon dose that was delivered to the sample during the experiment and that led to partial photoconversion (vide infra).

If one assumes that the excited state of the anionic green Dendra2 is obtained by ESPT, one should observe a component with the features of the emission spectrum of the anionic green form but with negative amplitude and a decay time of 3.4 or 40 ps. In contrast to the transient absorption experiments (vide infra), such a component is clearly not observed. One observes however two components with a positive amplitude, a decay time of 2.7 and 25 ps, and a maximum between 330 and 340 nm. The features of the DAS of these 2.7- and 25-ps components correspond to some extent to a combination of the anionic green and anionic red species.[5] This suggests that under the experimental conditions (pH 7.4) a fraction of the anionic green and anionic red molecules has additional fast nonradiative decay channels, e.g., relaxation possibly followed by energy transfer for the anionic green form.

One should note that the features of the DAS of the 25-ps component obtained for this sample (Figure 6) differ from those obtained for the partially photoconverted Dendra2 (Figure 3). This suggests that the 25-ps component is not only due to energy transfer but also to a conformational relaxation of the excited state of anionic green or the anionic red form. The smaller contribution of the energy transfer to the DAS of the 25-ps component in this sample can be due to the smaller extent of photoconversion (compared to the partially converted sample), leading to a smaller probability of dimer formation between an anionic green and an anionic red form.

A peculiar fast component of 1.8 ps with significant amplitude peaking at ∼600 nm is observed in the experiments performed at pH 7.4, indicating the presence of a species with an excited state located at lower energy than the red anionic form. This species has been previously detected in Dendra2 in steady-state measurements but only under very basic (pH 10) conditions and after strong light irradiation of the red form.[5] Similar red-shifted species have been earlier observed after intense illumination of DsRed in a stationary experiment at the ensemble[23,26,39] or single molecule[22,24] levels, and it was then referred to as a "super-red" (SR) configuration of the chromophore. In Dendra2, this is a short living species with very small emission quantum yield [about $3 \times 10^{-4}$ estimated from the decay time and the value of $k_f$ of the anionic red from ($1.4 \times 10^8$ $s^{-1}$)] at neutral pH conditions and thus impossible to be detected in stationary fluorescence experiments. One should note that the photo-Kolbe reaction proposed for the formation of the SR species can in principle also occur after excitation of the neutral green state. Actually, due to its larger energy content this state can be expected to have a much faster rate for electron transfer, as this process will be more exergonic. The radical (ions) formed in this process can then further initiate the $\beta$-elimination and proton shifts for the extension of the conjugation chain. This could possibly happen by hydrogen abstraction by the highly reactive primary alkyl radical obtained on the glutamate side chain.

It is striking to notice that among all red and red forms of photoconvertible fluorescent proteins, a SR species has been reported only for DsRed and Dendra2 up to now. An interesting structural feature that is common in these two FPs, whereas it is different for most of the other fluorescent proteins, is depicted in Figure 7. In almost all the structures of the anthozoan FPs known to date, the residue at position 70 in DsRed (66 in Dendra2) is an amino acid with a long side chain and bearing a charged amine group (lysine or arginine). Interestingly, this highly conserved residue has recently been identified as a probable proton donor to the excited chromophore.[37]

While in most FPs, including all green-to-red photoconvertible FPs except for Dendra2, this residue is directly interacting with the chromophore via the imidazolinone

carbonyl (Figures 7 C and S10B, Supporting Information), in a few exceptional cases, including DsRed and Dendra2, the interaction of this residue is not made with the chromophore but with the strictly conserved glutamate located in the vicinity of the chromophore via a saline bridge (Figures 7B and S10A, Supporting Information). This rare interaction found in DsRed and Dendra2 is only found in a very limited number of FPs structures—mKO,[58] mTFP1,[59] cmFP512,[60] and amFP486[61]—and is always favored by another interacting residue, Ser-197 in DsRed or Thr-69 in Dendra2, for example. The influence of this feature on the chromophore was already described with respect to a higher p$K_a$ and the blue-shift of the absorbance spectrum,[5] but its effect on the glutamate was neglected. In all known processes of photoactivation in wt-GFP,[27,29,30,62] PA-GFP,[63] or PAmCherry[33] or the oxidative redding of GFP,[64] an electron transfer from the glutamate (or redox partners in the case of the redding of GFP) to a positively charged chromophore is proposed to occur under intense illumination, leading to the decarboxylation of the glutamate via a photo-Kolbe reaction. Interestingly, while this decarboxylation is evidenced under intense irradiation conditions in DsRed,[26] none could be detected in its variant mOrange,[65] the structure of which shows the more classical direct interaction between the glutamate and the chromophore (Figure 7C). Altogether, these observations suggest that either the glutamate interacts directly with the nitrogen of the transiently charged chromophoric imidazolinone ring (as for GFP) or with a charged amine group of a strongly interacting residue (as for DsRed or Dendra2). This interaction could favor an electron transfer to the excited chromophore from the glutamate (photo-Kolbe reaction),[29] ultimately causing its decarboxylation; it could also be reversible under certain limits of irradiation and thus temporarily lead to a different charge distribution on the chromophore, a red-shift in its emission, and the observation of a SR species. Another possible explanation is that strong illumination can provoke the above-mentioned decarboxylation and that the peculiar arrangement in the chromophoric microenvironment favors the transient protonation of the imidazolinone ring of the chromophore and hence its transformation to a zwitterionic form whose emission was recently calculated to be red-shifted,[66] compatible with the observed SR species. The unstable double charged chromophore may serve as proton donor to the glutamate.

**Transient Absorption Experiments and Proposed Photoconversion Mechanism.** To understand better the effects of light excitation on the chromophore charge transfers, we can estimate the difference between the p$K_a$ values of the chromophore at the ground and excited states with eq 3[67]

$$pK_a^* = pK_a + \Delta E_{ex,solv}^{AH\rightarrow A^-}/\ln(10)RT \quad (3)$$

where p$K_a$ is the value measured at the ground-state, $\Delta E_{ex,solv}^{AH\rightarrow A^-}$ is the difference of the excitation energy of HA and $A^-$ (in J/mol) in the solvent used, $R$ is the gas constant (8.32 J $mol^{-1}$ $K^{-1}$), and $T$ is the temperature at which the p$K_a$ measurement was made.

For the green form of Dendra2, we measured at 25 °C a p$K_a$ of 7.1 with excitation peaks at 490 and 385 nm for the anionic and neutral forms of the chromophores, respectively. This gives a value of −4.55 for the p$K_a$*, which classifies the chromophore of Dendra2 as a photoacid and suggests that upon excitation of the neutral form, the green anionic chromophore can be immediately formed. The observation of green fluorescence upon excitation of the neutral form of Dendra2, indeed, previously led to proposing the existence of an ESPT in Dendra2 at the difference, for example, of EosFP, which does not fluoresce when its neutral form is excited.[5] Such a difference might originate from a different organization of the chromophoric microenvironment matrix in the two proteins and the existence of proton wires or proton escapes in Dendra2 as already deeply studied in GFP.[68−70] In this paper, we report the direct measurement of the ESPT in Dendra2, which indicates that its chromophore undergoes a Förster cycle. However, the green-to-red photoconversion is only visible when the neutral fraction is irradiated. The experiments above and literature data demonstrate that irradiation of the neutral state of the chromophore triggers a complex excited-state mechanism responsible for photoconversion from green to red,[1,19,20,71−73] as well as ESPT[5] leading to the anionic green species.

Complementary to the information obtained from stationary fluorescence and fluorescence up-conversion, femto- and picosecond transient absorption experiments were executed to elucidate those processes.

For a neutral green sample excited at pH 7.4 and 395 nm the transient absorption was recorded at 440 nm for a 12 ps time window where a negative signal with components of 273 fs (41%), 3.4 ps (54%), and 40 ps (5%) were obtained, all with the same negative sign (see Figure S7 of the Supporting Information; the long component was kept fixed during the fit analysis). Considering the stationary spectra (see Figure S9, Supporting Information), we can expect to observe at this wavelength induced emission of the neutral green form, yielding a negative signal, and if efficient photoconversion occurs on the time scale of the experiment, a growing in of the absorption of the neutral red or (the blue tail) of the anionic green occurs, the latter contributions both yielding a positive signal with decay time much longer than the time window of the experiment. As only a negative signal decaying to the background value was observed, the signal is apparently only due to induced emission of the neutral green species, and there is no indication of the formation of the ground state of the anionic green or neutral red in the time window of the experiment (12 ps). This does, however, not exclude that those species are formed in the excited state by an adiabatic process on this time scale. If this would be the case, only a very small population of the ground state will occur on the time scale of the experiment (12 ps) (Figure S7, Supporting Information) due to their long decay times of several hundreds of picoseconds to several nanoseconds. The 3.4- and 40-ps components then represent the decay of two different populations of the neutral green species. This interpretation agrees with the earlier conclusions drawn from the fluorescence decays of the green species obtained at 395 or 375 nm excitation and a time window of 50 ps (Figures 6, 7, and S6, Supporting Information) and 420 ps (Figure S8, Supporting Information). In the framework of this interpretation, the 273-fs component is due a vibrational relaxation or intramolecular vibrational redistribution of the excited neutral green species. This is quite possible as the probe wavelength is shorter than that of the emission maximum of the neutral green species.[5] An alternative assignment for this component could be a third population of neutral green excited states, where the first step[14] to the formation of the neutral red is the main decay process.

Transient absorption data of green Dendra2, with a probe wavelength between 490 and 590 nm with a time window of 45 ps, obtained upon excitation at 395 nm at pH 7.4 (Figure 8)

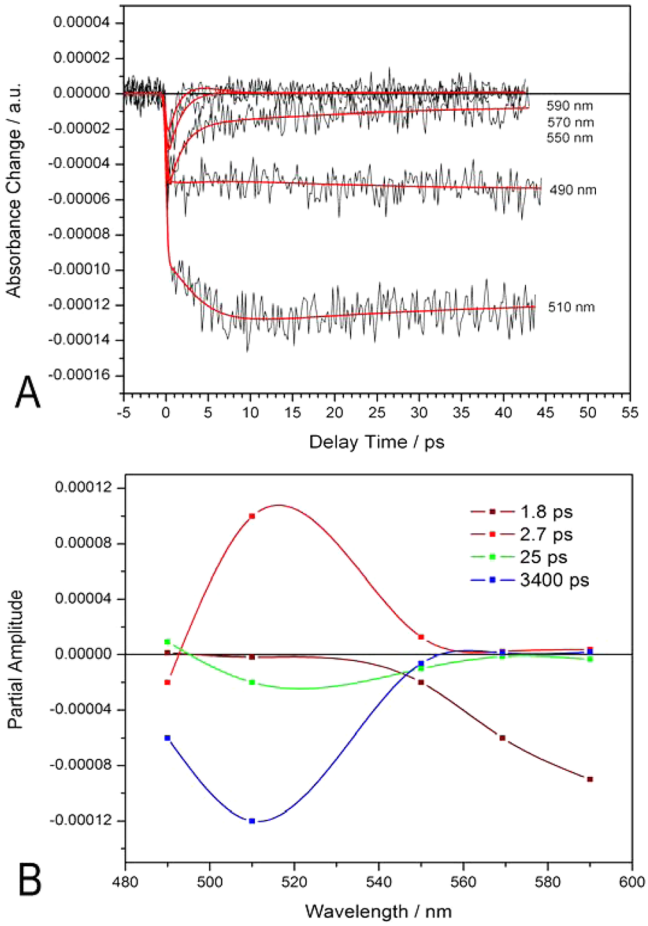


**Figure 8.** (A) Decay traces and corresponding fits obtained for green Dendra2 by femtosecond transient absorption in a 50 ps time window, ($\lambda_{exc}$ = 395 nm, $\lambda_{det}$ = 490−590 nm, pH 7.4). (B) The corresponding decay associated spectra. The 3400-ps component was kept fixed during the fit analysis.

could be analyzed as a sum of 4 exponentials with decay times of 1.8, 2.7, 25, and 3400 ps (the 3400-ps component was kept fixed during the fit analysis). While the components with decay times of 1.8, 25, and 3400 ps are always negative indicating ground state depletion or induced emission, the component with a decay time of 2.7 ps is everywhere positive except at 490 nm where it is slightly negative. When one of the decay times is fixed to 3.4 ps the 2.7-ps component disappears while the quality of the fit remains. In this case the features of the DAS of the 3.4-ps component resemble those of the 2.7-ps component. One should remark that already upon visual inspection the decay trace obtained for a probe wavelength of 510 nm clearly shows a growing in below 10 ps. The shape of the DAS of components with a decay time of 2.7 and 3400 ps are mirror images and match the emission spectrum of the anionic green and neutral red form. This suggests that the excited state of the emitting species is formed by an adiabatic process from the excited state of the neutral green species and with a time constant of 2.7−3.4 ps. Although the features of the DAS do not allow to decide whether the neutral red or anionic green state are formed by this adiabatic process starting from the excited state of the neutral green species the relative complex mechanism proposed in similar compounds for the conversion of a neutral green in a neutral red form[14] make it unlikely that this process occurs in 2.7 to 3.4 ps. Furthermore these mechanisms lead in a nonadiabatic way to a neutral red in its ground state, not in its $S_1$ state by an adiabatic process. Considering the extremely low value of quantum yield reported for the photoconversion to the neutral red ($10^{-3}$ to $10^{-4}$, reported for similar proteins[5]) this process would give rise in transient absorption experiments to a DAS with an amplitude that is several orders of magnitude lower than that of the ground state depletion and stimulated emission and will be extremely difficult to observe with this type of pump−probe experiments. This means that we can put an upper limit of ($5 \times 10^{-2}$)−0.1 on the quantum yield of this process. This does not contradict the effective photoconversion observed in the course of the transient absorption experiment. For a pump pulse of 150 $\mu$J at 395 nm impinging on a 1 mL of a $10^{-4}$ M solution of the neutral green with an absorbance of 0.4, $1.8 \times 10^{14}$ photons are absorbed per pulse by the neutral green. Hence for a pulse repetition rate of 1000 Hz, $1.8 \times 10^{17}$ photons are absorbed per second by a solution containing $6 \times 10^{16}$ protein molecules. If we assume that the absorbance is proportional with the concentration of the neutral green state it will take 330 s to obtain 67% conversion for a quantum yield of $10^{-3}$ for the photoconversion.

Hence, the 2.7 or 3.4 ps and 3.3 ns components most likely correspond to the adiabatic formation and the decay of the $S_1$ state of the anionic green form from the excited state of the neutral green form (Figure 9). As the kinetics of the excited

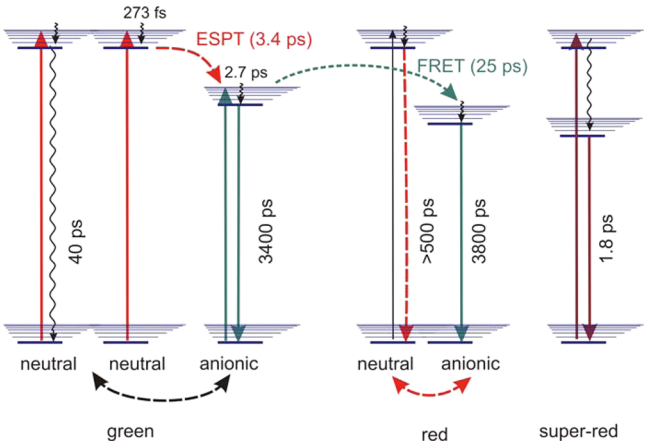


**Figure 9.** Kinetic scheme suggesting the excited state photophysical processes observed in Dendra2 upon 395 nm excitation.

state reaction to form the anionic green will involve, besides the ESPT itself, also vibrational relaxation and minor conformational changes with both positive contributions, it is possible that the signal attributed to the rise in fluorescence of the $S_1$ anionic green is canceled (figure 5). In principle, the decay of the $S_1$ state of the anionic green form should yield a positive signal at 490 nm due to absorption of the ground state of this species. However, considering its excited state decay time of 3.3 ns, this positive signal will only be observed in experiments on a time scale of 1 ns or more. At short wavelengths the 2.7- or 3.4-ps component goes much faster to zero than the 3.3-ns component, which can be attributed to the fact that at shorter wavelengths the former corresponds to a combination of the

decay of the induced emission of the neutral green (negative) and the growing in of the induced emission of the anionic green species (positive). Hence, upon decreasing the wavelength, the sign of this 2.7- or 3.4-ps component should change from positive to negative. This is indeed observed in Figure S7 (Supporting Information), where at 440 nm the 3.4-ps component has a negative sign. The 3.3-ns component is a combination of induced emission of the anionic green form (formed by either direct excitation of the anionic green present in the ground state at pH 7.4 or by ESPT after excitation of the neutral green form) and depletion of the ground state of the anionic green species present at pH 7.4 to the extent it is absorbing at 395 nm. Hence, for this component both contributions yield a negative signal. One should also note in Figure 8 that at the maximum of the 3.3-ns component the amplitude of the 3.3-ns component has the same size as that of the 2.7- or 3.4-ps component. This suggests that a majority of the excited anionic green species is formed by ESPT and that this species is formed only to a limited extend by direct absorption of the anionic green at 395 nm. In spite of the transient absorption experiments suggesting ESPT upon excitation of a sample of green Dendra2 at pH 7.4 and 395 nm, the excitation spectrum of the anionic green emission only has a very small shoulder between 400 and 350 nm. This means that the quantum yield to form the excited anionic green by ESPT is at maximum 10−20% and probably less. One of the reasons for this low quantum yield is the presence of two populations of neutral green, one with a 2.7−3.4-ps singlet decay time that contributes to the ESPT and one with a 40 ps singlet decay time that does not contribute to the ESPT. Figure 6 suggests that both components have a similar population. Hence 50% of the neutral green molecules cannot be involved in the ESPT. On basis of the transient absorption spectra, one would expect for the fluorescence up-conversion experiments on green Dendra2 upon excitation at 395 nm a 2.7−3.4-ps component with a negative sign and spectral features resembling those of the slowly decaying (3.3 ns) component. However, we observed a positive component with a decay time of 2.7−3.4 ps and spectral features resembling a combination of the anionic green and red forms. These components attributed to vibrational relaxation and/or minor conformational changes of anionic green and red species will obscure the expected negative signal.

Due to its small amplitude, it will be difficult to attribute the signal of the 25-ps component. It can possibly reflect a relaxation of the excited anionic green species. As we use a solution consisting still mainly of green Dendra2, it is less likely that we can attribute it to the energy transfer in a protein dimer.

The 1.8-ps component can be due to either ground-state depletion and induced emission of the super-red species (as in the up-conversion experiments) or (less likely) to the growing in of the absorption of a species intermediate in the formation of the neutral red.[14]

## ■ CONCLUSIONS

On the basis of the fluorescence time-resolved and transient absorption experiments on the femtosecond and picosecond time scale corroborated with literature data, the excited state processes found for Dendra2 suggest an ESPT in the neutral green species to form the anionic green species in a few picoseconds. The 3.4-ps time scale of the ESPT is similar to that found for DsRed (4 ps).[42] The population undergoing this process is distinct from the population of neutral green species decaying mainly by internal conversion. Which of those populations is involved in the triggering of the mechanism leading to a neutral red species remains to be established. It is also not evident whether the latter process can be identified with a population undergoing a radiationless decay in 200−300 fs, as the latter decay component can just represent a relaxation on the $S_1$ potential energy surface of the neutral green. Furthermore, the combination of fluorescence up-conversion and transient absorption experiments on the neutral green species indicates the presence of a least two and possibly three different populations decaying through different channels to the ground state. There is no evidence for the formation of an excited neutral red decaying on the picosecond time scale or for the formation of the ground state of a neutral red species on the picosecond time scale with efficiency larger than $(5 \times 10^{-2})$−0.1. Parallel investigations of fluorescent proteins with similar spectroscopic characteristics are ongoing and are expected to afford us a deeper insight into the photoconversion mechanism.

The presence of a "super-red" species with an emission spectrum in the 570−670 nm region and a decay time of 1.8 ps at neutral pH values was revealed. This super-red species is proposed to originate from a modification of the electron charges at the excited state between the chromophore and glutamate-215, a highly conserved residue in a peculiar interaction with the chromophores in both Dendra2 and DsRed, the only FPs in which a super-red species has been detected up to now. This reaction would become irreversible under intense irradiation, causing the photoinduced decarboxylation of this glutamate. In concentrated solutions, an energy transfer process between green anionic and red anionic chromophores was found to occur with a time constant of 25 ps. This work is not only important from a fundamental point of view to better understand the photophysics of the widely used fluorescent marker Dendra2 but it also stresses the importance of having stable monomers to avoid unexpected FRET effects when using green-to-red PCFPs even at micromolar concentration.

## ■ ASSOCIATED CONTENT

### Ⓢ Supporting Information

Additional experimental details and results on stationary absorption, emission, TCSPC, femtosecond transient absorption, and femtosecond up-conversion experiments are presented. This material is available free of charge via the Internet at http://pubs.acs.org.

## ■ AUTHOR INFORMATION

### Corresponding Author

*Phone: +33 4 38 78 95 67. Fax: +33 4 38 78 50 91. E-mail: virgile.adam@ibs.fr. Present address: Pixel Team, IBS, Institut de Biologie Structurale Jean-Pierre Ebel, CEA, CNRS, Université Joseph Fourier, 41 rue Jules Horowitz, F-38027 Grenoble, France, and Institut de Recherches en Technologies et Sciences pour le Vivant, iRTSV, Laboratoire de Physiologie Cellulaire et Végétale, CNRS/CEA/INRA/UJF, Grenoble, 38054, France.

### Notes

The authors declare no competing financial interest.

## ■ ACKNOWLEDGMENTS

Financial support of the "Fonds voor Wetenschappelijk Onderzoek FWO" (Grants G.0402.09, G0413.10, G0697.11,

G0197.11), the K.U. Leuven Research Fund (GOA 2011/03, "Interdisciplinair Onderzoek" IDO/07/010), the Flemish government (long term structural funding-Methusalem funding CASAS METH/08/04), and the Hercules foundation (HER/08/21) is gratefully acknowledged. B.M. is funded by a Ph.D. grant from the Agency for Innovation by Science and Technology (IWT) Flanders. Dr. Ryoko Ando is acknowledged for the analytical ultracentrifugation measurements of Dendra2. The authors are also indebted to Belspo through IAP VI/27 and VII/05.

## REFERENCES

(1) Gurskaya, N. G.; Verkhusha, V. V.; Shcheglov, A. S.; Staroverov, D. B.; Chepurnykh, T. V.; Fradkov, A. F.; Lukyanov, S.; Lukyanov, K. A. Engineering of a Monomeric Green-to-Red Photoactivatable Fluorescent Protein Induced by Blue Light. *Nat. Biotechnol.* **2006**, *24*, 461−465.

(2) Chudakov, D. M.; Lukyanov, S.; Lukyanov, K. A. Using Photoactivatable Fluorescent Protein Dendra2 to Track Protein Movement. *Biotechniques* **2007**, *42*, 553−563.

(3) Bulina, M. E.; Lukyanov, K. A.; Britanova, O. V.; Onichtchouk, D.; Lukyanov, S.; Chudakov, D. M. Chromophore-Assisted Light Inactivation (Cali) Using the Phototoxic Fluorescent Protein Killerred. *Nat. Protoc.* **2006**, *1*, 947−953.

(4) Baker, S. M.; Buckheit, R. W., 3rd; Falk, M. M. Green-to-Red Photoconvertible Fluorescent Proteins: Tracking Cell and Protein Dynamics on Standard Wide-Field Mercury Arc-Based Microscopes. *BMC Cell. Biol.* **2010**, *11*, 15.

(5) Adam, V.; Nienhaus, K.; Bourgeois, D.; Nienhaus, G. U. Structural Basis of Enhanced Photoconversion Yield in Green Fluorescent Protein-Like Protein Dendra2. *Biochemistry* **2009**, *48*, 4905−4915.

(6) Chudakov, D. M.; Lukyanov, S.; Lukyanov, K. A. Tracking Intracellular Protein Movements Using Photoswitchable Fluorescent Proteins Ps-Cfp2 and Dendra2. *Nat. Protoc.* **2007**, *2*, 2024−2032.

(7) Gould, T. J.; Gunewardene, M. S.; Gudheti, M. V.; Verkhusha, V. V.; Yin, S. R.; Gosse, J. A.; Hess, S. T. Nanoscale Imaging of Molecular Positions and Anisotropies. *Nat. Methods* **2008**, *5*, 1027−1030.

(8) Niu, L.; Yu, J. Investigating Intracellular Dynamics of Ftsz Cytoskeleton with Photoactivation Single-Molecule Tracking. *Biophys. J.* **2008**, *95*, 2009−2016.

(9) Watanabe, S.; Punge, A.; Hollopeter, G.; Willig, K. I.; Hobson, R. J.; Davis, M. W.; Hell, S. W.; Jorgensen, E. M. Protein Localization in Electron Micrographs Using Fluorescence Nanoscopy. *Nat. Methods* **2011**, *8*, 80−84.

(10) Heilemann, M.; Dedecker, P.; Hofkens, J.; Sauer, M. Photoswitches: Key Molecules for Subdiffraction-Resolution Fluorescence Imaging and Molecular Quantification. *Laser Photon Rev.* **2009**, *3*, 180−202.

(11) Flors, C.; Hotta, J.; Uji-i, H.; Dedecker, P.; Ando, R.; Mizuno, H.; Miyawaki, A.; Hofkens, J. A Stroboscopic Approach for Fast Photoactivation−Localization Microscopy with Dronpa Mutants. *J. Am. Chem. Soc.* **2007**, *129*, 13970−13977.

(12) Dedecker, P.; Hotta, J.; Flors, C.; Sliwa, M.; Uji-i, H.; Roeffaers, M. B.; Ando, R.; Mizuno, H.; Miyawaki, A.; Hofkens, J. Subdiffraction Imaging through the Selective Donut-Mode Depletion of Thermally Stable Photoswitchable Fluorophores: Numerical Analysis and Application to the Fluorescent Protein Dronpa. *J. Am. Chem. Soc.* **2007**, *129*, 16132−16141.

(13) Lehmann, M.; Rocha, S.; Mangeat, B.; Blanchet, F.; Uji, I. H.; Hofkens, J.; Piguet, V. Quantitative Multicolor Super-Resolution Microscopy Reveals Tetherin HIV-1 Interaction. *PLoS Pathog.* **2011**, *7*, e1002456.

(14) Wachter, R. M.; Watkins, J. L.; Kim, H. Mechanistic Diversity of Red Fluorescence Acquisition by Gfp-like Proteins. *Biochemistry* **2010**, *49*, 7417−7427.

(15) Li, X.; Chung, L. W.; Mizuno, H.; Miyawaki, A.; Morokuma, K. Competitive Mechanistic Pathways for Green-to-Red Photoconversion in the Fluorescent Protein Kaede: A Computational Study. *J. Phys. Chem. B* **2010**, *114*, 16666−16675.

(16) Tsutsui, H.; Shimizu, H.; Mizuno, H.; Nukina, N.; Furuta, T.; Miyawaki, A. The E1 Mechanism in Photo-Induced Beta-Elimination Reactions for Green-to-Red Conversion of Fluorescent Proteins. *Chem. Biol.* **2009**, *16*, 1140−1147.

(17) Hayashi, I.; Mizuno, H.; Tong, K. I.; Furuta, T.; Tanaka, F.; Yoshimura, M.; Miyawaki, A.; Ikura, M. Crystallographic Evidence for Water-Assisted Photo-Induced Peptide Cleavage in the Stony Coral Fluorescent Protein Kaede. *J. Mol. Biol.* **2007**, *372*, 918−926.

(18) Nienhaus, K.; Nienhaus, G. U.; Wiedenmann, J.; Nar, H. Structural Basis for Photo-Induced Protein Cleavage and Green-to-Red Conversion of Fluorescent Protein Eosfp. *Proc. Natl. Acad. Sci. U. S. A.* **2005**, *102*, 9156−9159.

(19) Mizuno, H.; Mal, T. K.; Tong, K. I.; Ando, R.; Furuta, T.; Ikura, M.; Miyawaki, A. Photo-Induced Peptide Cleavage in the Green-to-Red Conversion of a Fluorescent Protein. *Mol. Cell* **2003**, *12*, 1051−1058.

(20) Lelimousin, M.; Adam, V.; Nienhaus, G. U.; Bourgeois, D.; Field, M. J. Photoconversion of the Fluorescent Protein Eosfp: A Hybrid Potential Simulation Study Reveals Intersystem Crossings. *J. Am. Chem. Soc.* **2009**, *131*, 16814−16823.

(21) Adam, V.; Moeyaert, B.; David, C. C.; Mizuno, H.; Lelimousin, M.; Dedecker, P.; Ando, R.; Miyawaki, A.; Michiels, J.; Engelborghs, Y.; et al. Rational Design of Photoconvertible and Biphotochromic Fluorescent Proteins for Advanced Microscopy Applications. *Chem. Biol.* **2011**, *18*, 1241−1251.

(22) Cotlet, M.; Hofkens, J.; Habuchi, S.; Dirix, G.; Van Guyse, M.; Michiels, J.; Vanderleyden, J.; De Schryver, F. C. Identification of Different Emitting Species in the Red Fluorescent Protein Dsred by Means of Ensemble and Single-Molecule Spectroscopy. *Proc. Natl. Acad. Sci. U. S. A.* **2001**, *98*, 14398−14403.

(23) Malvezzi-Campeggi, F.; Jahnz, M.; Heinze, K. G.; Dittrich, P.; Schwille, P. Light-Induced Flickering of Dsred Provides Evidence for Distinct and Interconvertible Fluorescent States. *Biophys. J.* **2001**, *81*, 1776−1785.

(24) Blum, C.; Meixner, A. J.; Subramaniam, V. Single Oligomer Spectra Probe Chromophore Nanoenvironments of Tetrameric Fluorescent Proteins. *J. Am. Chem. Soc.* **2006**, *128*, 8664−8670.

(25) Blum, C.; Meixner, A. J.; Subramaniam, V. Spectral Versatility of Single Reef Coral Fluorescent Proteins Detected by Spectrally-Resolved Single Molecule Spectroscopy. *ChemPhysChem* **2008**, *9*, 310−315.

(26) Habuchi, S.; Cotlet, M.; Gensch, T.; Bednarz, T.; Haber-Pohlmeier, S.; Rozenski, J.; Dirix, G.; Michiels, J.; Vanderleyden, J.; Heberle, J.; et al. Evidence for the Isomerization and Decarboxylation in the Photoconversion of the Red Fluorescent Protein Dsred. *J. Am. Chem. Soc.* **2005**, *127*, 8977−8984.

(27) Bell, A. F.; Stoner-Ma, D.; Wachter, R. M.; Tonge, P. J. Light-Driven Decarboxylation of Wild-Type Green Fluorescent Protein. *J. Am. Chem. Soc.* **2003**, *125*, 6919−6926.

(28) Piatkevich, K. D.; Verkhusha, V. V. Advances in Engineering of Fluorescent Proteins and Photoactivatable Proteins with Red Emission. *Curr. Opin. Chem. Biol.* **2010**, *14*, 23−29.

(29) van Thor, J. J.; Gensch, T.; Hellingwerf, K. J.; Johnson, L. N. Phototransformation of Green Fluorescent Protein with UV and Visible Light Leads to Decarboxylation of Glutamate 222. *Nat. Struct. Biol.* **2002**, *9*, 37−41.

(30) van Thor, J. J.; Georgiev, G. Y.; Towrie, M.; Sage, J. T. Ultrafast and Low Barrier Motions in the Photoreactions of the Green Fluorescent Protein. *J. Biol. Chem.* **2005**, *280*, 33652−33659.

(31) Chudakov, D. M.; Verkhusha, V. V.; Staroverov, D. B.; Souslova, E. A.; Lukyanov, S.; Lukyanov, K. A. Photoswitchable Cyan Fluorescent Protein for Protein Tracking. *Nat. Biotechnol.* **2004**, *22*, 1435−1439.

(32) Henderson, J. N.; Gepshtein, R.; Heenan, J. R.; Kallio, K.; Huppert, D.; Remington, S. J. Structure and Mechanism of the Photoactivatable Green Fluorescent Protein. *J. Am. Chem. Soc.* **2009**, *131*, 4176−4177.

(33) Subach, F. V.; Malashkevich, V. N.; Zencheck, W. D.; Xiao, H.; Filonov, G. S.; Almo, S. C.; Verkhusha, V. V. Photoactivation Mechanism of Pamcherry Based on Crystal Structures of the Protein in the Dark and Fluorescent States. *Proc. Natl. Acad. Sci. U. S. A.* **2009**, *106*, 21097−21102.
(34) Valentin, G.; Verheggen, C.; Piolot, T.; Neel, H.; Coppey-Moisan, M.; Bertrand, E. Photoconversion of Yfp into a Cfp-like Species During Acceptor Photobleaching Fret Experiments. *Nat. Methods* **2005**, *2*, 801.
(35) Adam, V.; Carpentier, P.; Violot, S.; Lelimousin, M.; Darnault, C.; Nienhaus, G. U.; Bourgeois, D. Structural Basis of X-ray-Induced Transient Photobleaching in a Photoactivatable Green Fluorescent Protein. *J. Am. Chem. Soc.* **2009**, *131*, 18063−18065.
(36) McAnaney, T. B.; Zeng, W.; Doe, C. F.; Bhanji, N.; Wakelin, S.; Pearson, D. S.; Abbyad, P.; Shi, X.; Boxer, S. G.; Bagshaw, C. R. Protonation, Photobleaching, and Photoactivation of Yellow Fluorescent Protein (Yfp 10c): A Unifying Mechanism. *Biochemistry* **2005**, *44*, 5510−5524.
(37) Roy, A.; Field, M. J.; Adam, V.; Bourgeois, D. The Nature of Transient Dark States in a Photoactivatable Fluorescent Protein. *J. Am. Chem. Soc.* **2011**, *133*, 18586−18589.
(38) Royant, A.; Noirclerc-Savoye, M. Stabilizing Role of Glutamic Acid 222 in the Structure of Enhanced Green Fluorescent Protein. *J. Struct. Biol.* **2011**, *174*, 385−390.
(39) Bonsma, S.; Gallus, J.; Konz, F.; Purchase, R.; Volker, S. Light-Induced Conformational Changes and Energy Transfer in Red Fluorescent Protein. *J. Lumin.* **2004**, *107*, 203−212.
(40) Mizuno, H.; Dedecker, P.; Ando, R.; Fukano, T.; Hofkens, J.; Miyawaki, A. Higher Resolution in Localization Microscopy by Slower Switching of a Photochromic Protein. *Photochem. Photobiol. Sci.* **2010**, *9*, 239−248.
(41) Lide, D. R. *CRC Handbook of Chemistry and Physics: A Ready-Reference Book of Chemical and Physical Data*, 84th ed.; CRC-Press: Boca Raton, FL, 2003.
(42) Maus, M.; Rousseau, E.; Cotlet, M.; Schweitzer, G.; Hofkens, J.; Van der Auweraer, M.; De Schryver, F. C.; Krueger, A. New Picosecond Laser System for Easy Tunability over the Whole Ultraviolet/Visible/Near Infrared Wavelength Range Based on Flexible Harmonic Generation and Optical Parametric Oscillation. *Rev. Sci. Instrum.* **2001**, *72*, 36−40.
(43) Boens, N.; Qin, W.; Basaric, N.; Hofkens, J.; Ameloot, M.; Pouget, J.; Lefevre, J. P.; Valeur, B.; Gratton, E.; vandeVen, M.; et al. Fluorescence Lifetime Standards for Time and Frequency Domain Fluorescence Spectroscopy. *Anal. Chem.* **2007**, *79*, 2137−2149.
(44) Program developed in a cooperation between the Management of Technology Institute (Belarusian State University) and The Division of Photochemistry and Spectroscopy (University of Leuven).
(45) O'Connor, D. V.; Phillips, D. *Time-Correlated Single Photon Counting*; Academic Press: London, 1984.
(46) Karni, Y.; Jordens, S.; De Belder, G.; Schweitzer, G.; Hofkens, J.; Gensch, T.; Maus, M.; De Schryver, F. C.; Hermann, A.; Mullen, K. Intramolecular Evolution from a Locally Excited State to an Excimer-Like State in a Multichromophoric Dendrimer Evidenced by a Femotosecond Fluorescence Upconversion Study. *Chem. Phys. Lett.* **1999**, *310*, 73−78.
(47) Habuchi, S.; Ando, R.; Dedecker, P.; Verheijen, W.; Mizuno, H.; Miyawaki, A.; Hofkens, J. Reversible Single-Molecule Photoswitching in the Gfp-Like Fluorescent Protein Dronpa. *Proc. Natl. Acad. Sci. U. S. A.* **2005**, *102*, 9511−9516.
(48) Fron, E.; Flors, C.; Schweitzer, G.; Habuchi, S.; Mizuno, H.; Ando, R.; Schryver, F. C.; Miyawaki, A.; Hofkens, J. Ultrafast Excited-State Dynamics of the Photoswitchable Protein Dronpa. *J. Am. Chem. Soc.* **2007**, *129*, 4870−4871.
(49) Hosoi, H.; Mizuno, H.; Miyawaki, A.; Tahara, T. Competition between Energy and Proton Transfer in Ultrafast Excited-State Dynamics of an Oligomeric Fluorescent Protein Red Kaede. *J. Phys. Chem. B* **2006**, *110*, 22853−22860.
(50) Blum, C.; Subramaniam, V. Single-Molecule Spectroscopy of Fluorescent Proteins. *Anal. Bioanal. Chem.* **2009**, *393*, 527−541.
(51) Heikal, A. A.; Hess, S. T.; Baird, G. S.; Tsien, R. Y.; Webb, W. W. Molecular Spectroscopy and Dynamics of Intrinsically Fluorescent Proteins: Coral Red (Dsred) and Yellow (Citrine). *Proc. Natl. Acad. Sci. U. S. A.* **2000**, *97*, 11996−12001.
(52) Lounis, B.; Deich, J.; Rosell, F. I.; Boxer, S. G.; Moerner, W. E. Photophysics of Dsred, a Red Fluorescent Protein, from the Ensemble to the Single-Molecule Level. *J. Phys. Chem. B* **2001**, *105*, 5048−5054.
(53) Verkhusha, V. V.; Chudakov, D. M.; Gurskaya, N. G.; Lukyanov, S.; Lukyanov, K. A. Common Pathway for the Red Chromophore Formation in Fluorescent Proteins and Chromoproteins. *Chem. Biol.* **2004**, *11*, 845−854.
(54) Förster, T. 10th Spiers Memorial Lecture. Transfer Mechanisms of Electronic Excitation. *Discuss. Faraday Soc.* **1959**, *27*, 7−17.
(55) Wiedenmann, J.; Vallone, B.; Renzi, F.; Nienhaus, K.; Ivanchenko, S.; Rocker, C.; Nienhaus, G. U. Red Fluorescent Protein Eqfp611 and Its Genetically Engineered Dimeric Variants. *J. Biomed. Opt.* **2005**, *10*, 14003.
(56) Lessard, G. A.; Habuchi, S.; Werner, J. H.; Goodwin, P. M.; De Schryver, F.; Hofkens, J.; Cotlet, M. Probing Dimerization and Intraprotein Fluorescence Resonance Energy Transfer in a Far-Red Fluorescent Protein from the Sea Anemone *Heteractis crispa*. *J. Biomed. Opt.* **2008**, *13*, 031212.
(57) Braslavsky, S. E.; Fron, E.; Rodriguez, H. B.; Roman, E. S.; Scholes, G. D.; Schweitzer, G.; Valeur, B.; Wirz, J. Pitfalls and Limitations in the Practical Use of Forster's Theory of Resonance Energy Transfer. *Photochem. Photobiol. Sci.* **2008**, *7*, 1444−1448.
(58) Kikuchi, A.; Fukumura, E.; Karasawa, S.; Mizuno, H.; Miyawaki, A.; Shiro, Y. Structural Characterization of a Thiazoline-Containing Chromophore in an Orange Fluorescent Protein, Monomeric Kusabira Orange. *Biochemistry* **2008**, *47*, 11573−11580.
(59) Ai, H. W.; Olenych, S. G.; Wong, P.; Davidson, M. W.; Campbell, R. E. Hue-Shifted Monomeric Variants of Clavularia Cyan Fluorescent Protein: Identification of the Molecular Determinants of Color and Applications in Fluorescence Imaging. *BMC Biol.* **2008**, *6*, 13.
(60) Nienhaus, K.; Renzi, F.; Vallone, B.; Wiedenmann, J.; Nienhaus, G. U. Exploring Chromophore−Protein Interactions in Fluorescent Protein Cmfp512 from *Cerianthus membranaceus*: X-Ray Structure Analysis and Optical Spectroscopy. *Biochemistry* **2006**, *45*, 12942−12953.
(61) Henderson, J. N.; Remington, S. J. Crystal Structures and Mutational Analysis of Amfp486, a Cyan Fluorescent Protein from *Anemonia majano*. *Proc. Natl. Acad. Sci. U. S. A.* **2005**, *102*, 12712−12717.
(62) van Thor, J. J.; Sage, J. T. Charge Transfer in Green Fluorescent Protein. *Photochem. Photobiol. Sci.* **2006**, *5*, 597−602.
(63) Patterson, G. H.; Lippincott-Schwartz, J. A Photoactivatable Gfp for Selective Photolabeling of Proteins and Cells. *Science* **2002**, *297*, 1873−1877.
(64) Bogdanov, A. M.; Mishin, A. S.; Yampolsky, I. V.; Belousov, V. V.; Chudakov, D. M.; Subach, F. V.; Verkhusha, V. V.; Lukyanov, S.; Lukyanov, K. A. Green Fluorescent Proteins Are Light-Induced Electron Donors. *Nat. Chem. Biol.* **2009**, *5*, 459−461.
(65) Shaner, N. C.; Lin, M. Z.; McKeown, M. R.; Steinbach, P. A.; Hazelwood, K. L.; Davidson, M. W.; Tsien, R. Y. Improving the Photostability of Bright Monomeric Orange and Red Fluorescent Proteins. *Nat. Methods* **2008**, *5*, 545−551.
(66) Imhof, P. Computational Study of Absorption Spectra of the Photoconvertible Fluorescent Protein Eosfp in Different Protonation States. *J. Chem. Theory Comput.* **2012**, *8*, 4828−4836.
(67) Baranov, M. S.; Lukyanov, K. A.; Borissova, A. O.; Shamir, J.; Kosenkov, D.; Slipchenko, L. V.; Tolbert, L. M.; Yampolsky, I. V.; Solntsev, K. M. Conformationally Locked Chromophores as Models of Excited-State Proton Transfer in Fluorescent Proteins. *J. Am. Chem. Soc.* **2012**, *134*, 6025−6032.
(68) Agmon, N. Proton Pathways in Green Fluorescence Protein. *Biophys. J.* **2005**, *88*, 2452−2461.

(69) Leiderman, P.; Huppert, D.; Agmon, N. Transition in the Temperature-Dependence of Gfp Fluorescence: From Proton Wires to Proton Exit. *Biophys. J.* **2006**, *90*, 1009−1018.
(70) Shinobu, A.; Palm, G. J.; Schierbeek, A. J.; Agmon, N. Visualizing Proton Antenna in a High-Resolution Green Fluorescent Protein Structure. *J. Am. Chem. Soc.* **2010**, *132*, 11093−11102.
(71) Ando, R.; Hama, H.; Yamamoto-Hino, M.; Mizuno, H.; Miyawaki, A. An Optical Marker Based on the UV-Induced Green-to-Red Photoconversion of a Fluorescent Protein. *Proc. Natl. Acad. Sci. U. S. A.* **2002**, *99*, 12651−12656.
(72) Tsutsui, H.; Karasawa, S.; Shimizu, H.; Nukina, N.; Miyawaki, A. Semi-Rational Engineering of a Coral Fluorescent Protein into an Efficient Highlighter. *EMBO Rep.* **2005**, *6*, 233−238.
(73) Wiedenmann, J.; Ivanchenko, S.; Oswald, F.; Schmitt, F.; Rocker, C.; Salih, A.; Spindler, K. D.; Nienhaus, G. U. Eosfp, a Fluorescent Marker Protein with UV-Inducible Green-to-Red Fluorescence Conversion. *Proc. Natl. Acad. Sci. U. S. A.* **2004**, *101*, 15905−15910.